View Article Online
View Journal

Organic & Biomolecular Chemistry

Accepted Manuscript

This article can be cited before page numbers have been issued, to do this please use: W. G. Kim, S. Baek, S. Y. Jeong, D. Nam, J. H. Jeon, W. Choe, M. Baik and S. Y. Hong, *Org. Biomol. Chem.*, 2020, DOI: 10.1039/D0OB00579G.

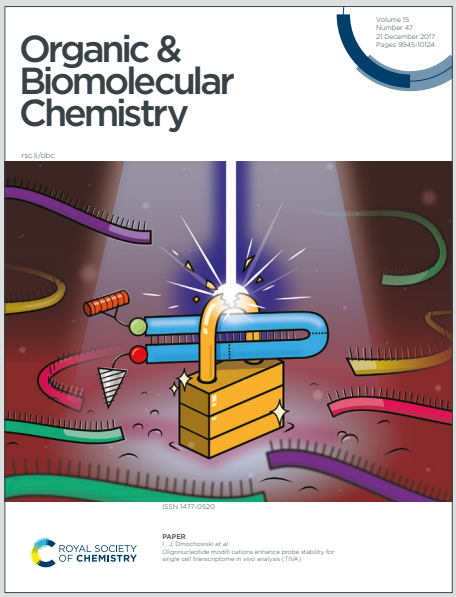

ROYAL SOCIETY OF CHEMISTRY

rsc.li/obc

View Article Online
DOI: 10.1039/D0OB00579G

PAPER

Chemo- and regioselective click reactions through nickel-catalyzed azide–alkyne cycloaddition†

Received 00th January 20xx,
Accepted 00th January 20xx

DOI: 10.1039/x0xx00000x

Woo Gyum Kim,§[a] Seung-yeol Baek,§[bc] Seo Yeong Jeong,[a] Dongsik Nam,[d] Ji Hwan Jeon,[a] Wonyoung Choe,[d] Mu-Hyun Baik*[bc] and Sung You Hong*[ad]

Metal-catalyzed cycloaddition is an expeditious synthetic route to functionalized heterocyclic frameworks. However, achieving reactivity-controlled metal-catalyzed azide–alkyne cycloadditions from competing internal alkynes has been challenging. Herein, we report a nickel-catalyzed [3 + 2] cycloaddition of unsymmetrical alkynes with organic azides to afford functionalized 1,2,3-triazoles with excellent regio- and chemoselectivity control. Terminal alkynes and cyanoalkynes afford 1,5-disubstituted triazoles and 1,4,5-trisubstituted triazoles bearing a 4-cyano substituent, respectively. Thioalkynes and ynamides exhibit inverse regioselectivity compared with terminal alkynes and cyanoalkynes, affording 1,4,5-trisubstituted triazoles with 5-thiol and 5-amide substituents, respectively. Density functional theory calculations are performed for the elucidation of the reaction mechanism. The computed mechanism suggests that a nickellacyclopropene intermediate is generated by the oxidative addition of the alkyne substrate to the Ni(0)-Xantphos catalyst, and the subsequent C–N coupling of this intermediate with an azide is responsible for the chemo- and regioselectivity.

Introduction

Controlled transformations of substrates to construct targeted structures have constituted key synthetic topics.[1] Reactivity or selectivity differentiation between competing functional moieties can allow atom- and step-economical bond-formation routes, which avoid tedious multi-step processes often associated with sophisticated protecting group chemistry. Cycloaddition reactions are powerful synthetic tools for the straightforward modular construction of heterocycles that utilizes readily available molecular building blocks.[2] Frontier orbital interactions between dipoles and dipolarophiles are of particular importance in determining reactivity preferences and regiochemical outcome. However, the Huisgen 1,3-dipolar cycloaddition often gives rise to a mixture of regioisomeric five-membered rings. While thermally promoted cycloadditions feature concerted bond formation via a single transition state, transition-metal-catalyzed variants employ a series of coordination modes. The preferential orientations of active metal moieties towards unsymmetrical π-components allow high levels of regioselectivity and enhanced chemical reactivity.[3] Copper-catalyzed azide–alkyne cycloaddition (CuAAC), a prominent example of click chemistry, involves stepwise carbon–nitrogen bond formation via a copper acetylide intermediate to give exclusively 1,4-disubstituted 1,2,3-triazoles.[4-9] As a complementary method, RuAAC reactions commonly employing [Cp*RuCl] complexes produce 1,5-disubstituited or 1,4,5-trisubstituted triazoles from terminal and internal alkynes via ruthenacycle complexes.[10-16] RhAAC[17-20] and IrAAC[21-25] have been effectively utilized for internal alkynes bearing heteroatoms with high levels of regioselectivity. Recently, we reported the nickel-catalyzed AAC approach to access 1,5-regioisomers under ambient conditions.[26] This NiAAC chemistry was applied to the construction of non-natural amino acids or glycoconjugates, without the implementation of the Schlenk technique, a glovebox, or degassed solvent.

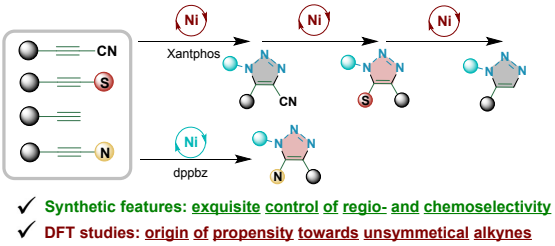

Scheme 1 Combined experimental and computational studies of NiAAC reactions using competing unsymmetrical acetylenes.

The propensity of organic azides to distinguish specific acetylene motifs over competing alkynes can be exploited to exert chemoselectivity.[27-36] Successive click protocols that merge strain-promoted cycloaddition (SPAAC) and CuAAC have been demonstrated on the basis of reactivity differences between cyclooctynes and acetylenes.[27,28] The presence of

[a] School of Energy and Chemical Engineering, Ulsan National Institute of Science and Technology, Ulsan 44919, Republic of Korea. E-mail: syhong@unist.ac.kr
[b] Department of Chemistry, Korea Advanced Institute of Science and Technology, Daejeon 34141, Republic of Korea. E-mail: mbaik2805@kaist.ac.kr
[c] Center for Catalytic Hydrocarbon Functionalizations, Institute for Basic Science (IBS), Daejeon 34141, Republic of Korea.
[d] Department of Chemistry, Ulsan National Institute of Science and Technology, Ulsan 44919, Republic of Korea.
† Electronic supplementary information (ESI) available: Experimental procedures, spectral data, single-crystal X-ray data. See DOI: 10.1039/x0xx00000x
§ These authors contributed equally to this work.

protecting groups, such as in trimethylsilyl (TMS)-substituted acetylenes, has been shown to be advantageous in sequential-click strategies,[29-31] and chemoselective CuAAC reactions of various terminal alkynes or iodoalkynes have also been investigated.[32-36] Despite these advances, establishing a unified synthetic approach to access 1,4,5-trisubstituted triazoles from different internal alkynes has remained as a challenging topic. Herein, we disclose highly regio- and chemoselective NiAAC reactions employing a variety of internal and terminal alkyne components including cyanoalkynes, ynamides, thioalkynes, and phenylacetylenes. DFT calculations were performed in order to elucidate the mechanism leading to the observed reactivity preference and regiochemical outcome, which were dependent on the alkyne components (Scheme 1).

Results and discussion

Cyanoalkynes, thioalkynes, and ynamides were deemed as ideal substrates for the study, as these heteroatom-substituted internal alkynes are readily accessible and are electronically polarized structures that are commonly employed in RuAAC, RhAAC, and/or IrAAC. Under the catalytic conditions using the Cp_2Ni/P-ligand, the representative cyanoalkyne **2a**, thioalkyne **3a**, and ynamide **4a** exhibited facile reactivity with benzyl azide **1a**, to furnish fully substituted 1,2,3-triazoles (Table 1). After surveying a diverse set of ligands (see the ESI†; Table S1), we found that the bidentate phosphine ligands,[37] Xantphos or dppbz, were the optimal ligands. Xantphos ligand effectively facilitates the cycloadditions of **2a** and **3a** to afford the corresponding triazoles with excellent, but reversed regiochemical outcomes of 13:1 for 4-cyano-1,2,3-triazole **5aa** (Table 1, entries 1 and 2), and exclusive formation of 5-thio-1,2,3-triazole **6aa** (entries 3 to 5). Interestingly, dppbz promoted the efficient dipolar cycloaddition of **4a** to give the 5-amido-1,2,3-triazole **7aa** (entries 6 to 8). The NiAAC reactions were compatible with various reaction media, air, and moisture. The reactions proceeded well in DCM, tetrahydrofuran, DMF, and toluene (see also Table S2).

Table 1 Optimization of reaction conditions[a]

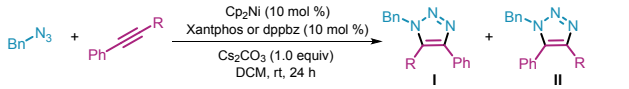

1a — **2a**, R = CN; **3a**, R = SBn; **4a**, R = 2-oxazolidinone → **5aa**, R = CN; **6aa**, R = SBn; **7aa**, R = 2-oxazolidinone

Entry	Alkyne, R	Ligand	Yield (%)[b] I	Yield (%)[b] II
1	**2a, CN**	**Xantphos**	**7**	**91**
2	**2a**, CN	dppbz	3	47
3	**3a**, SBn	dppbz	20	-
4	**3a**, SBn	Xantphos	73	-
5[c]	**3a, SBn**	**Xantphos**	**91**	**-**
6	**4a**, 2-oxazolidinone	Xantphos	45	15
7[d]	**4a**, 2-oxazolidinone	dppbz	78	5
8[e]	**4a, 2-oxazolidinone**	**dppbz**	**89**	**5**

[a] Reaction conditions: **1a** (0.38 mmol), **2a–4a** (0.46 mmol, 1.2 equiv), Cp_2Ni (10 mol %), P-ligand (10 mol %), Cs_2CO_3 (1.0 equiv) in DCM (2.0 mL) at rt under air for 24 h. [b] Isolated yield. [c] Cp_2Ni (20 mol %), Xantphos (20 mol %). [d] Reaction in toluene (2.0 mL). [e] Cp_2Ni (20 mol %), dppbz (20 mol %) in toluene (2.0 mL). Bn, benzyl; Ph, phenyl; Cp, cyclopentadienyl; DCM, dichloromethane; dppbz, 1,2-bis(diphenylphosphino)benzene.

With these successful prototype reactions in hand, we evaluated the scope of the organic azide and unsymmetrical internal alkyne substrates under the optimized conditions, as summarized in Table 2. A variety of organic azides (**1a–1i**), cyanoalkynes (**2a–2e**), thioalkynes (**3a–3h**), and ynamides (**4a–4l**) were utilized to examine the generality of the NiAAC. The resulting triazole structures **5–7** were examined and characterized by 1D- and 2D NMR techniques, including HSQC, HMBC, and/or NOESY, and single-crystal X-ray analysis, as detailed in the ESI† (Sections VI and VII). Organic azides (**1a–1g**) and cyanoalkyne **2a** proficiently undergo the dipolar cycloadditions to produce the corresponding 4-cyano-1,2,3-triazoles (**5aa–5ga**) in high isolated yields (79–95%) and excellent regioselectivity (11.3:1–30:1 ratio). The regioselectivity between 4-cyano-1,2,3-triazoles and their regioisomers, 5-cyano-1,2,3-triazoles, depends on cyanoalkyne polarization. Erosion in regiochemical outcomes (3.6:1–5.8:1 ratio) was observed for triazoles (**5ac–5ae**), when coupled with the corresponding cyanoalkynes bearing electron-withdrawing groups (**2c–2e**). In sharp contrast, enhanced regioselectivity (24.5:1 ratio) was recorded for **5ab**, bearing the *p*-OMePh group. These results suggest that inductive effects may interfere with nitrile groups to alter the polarization of the carbon–carbon triple bond. To our delight, organic azides **1** and thioalkynes **3** afforded the corresponding 5-thio-1,2,3-triazoles **6** with exclusive regioselectivity with various functional groups including fluoro-, trifluoro-, methoxy-, and cyano-, and nitro moieties being fully tolerated. Interestingly, regioselectivity is not sensitive to steric effects. Cycloadditions of azides **1** with ynamides **4**, bearing carbamates and sulfonamides, were also evaluated to afford 5-amido-triazoles **7**. In these reactions, sterics exerted a significant influence on ynamide conjugation, and sterically congested triazoles (**7ac**, **7ah**) could not be prepared. *p*-OMe-Substituted **4g** produced the 5-amido triazole **7ag** with poor selectivity (5.7:1 ratio), in contrast to substrates **4e** and **4f**. Furthermore, gram-scale tolerance was representatively demonstrated for the distinct internal alkynes (**5cb**, **6ah**, and **7ab**). Yet, the substrate scope is limited to benzyl- or alkyl azides and mostly aryl-bearing alkynes. The design of well-defined catalytic systems will be the critical step for extended NiAAC studies.

Precise reactivity control toward specific alkyne substrates is essential for designing reliable and predictable NiAAC methods. Thus, we performed competition experiments in order to rank reactive alkyne components in the NiAAC methodology. An equimolar mixture of binary alkyne components and organic azide was reacted under optimized conditions. Substituents responsible for tuning the electronic character of the alkyne components were included, in order to examine their influence on reactivity. Cyanoalkyne **2a** exhibited

View Article Online
DOI: 10.1039/D0OB00579C

superior reactivity compared to phenylacetylene, to give 4-cyano-triazole in 91% yield (Fig. 1A). Evaluation of electron-donating (*p*-OMePh) and electron-withdrawing (*p*-CNPh) moieties on the cyanoalkynes (**2b**, **2c**) indicated marginal differences. Competition tests of thioalkyne **3a** and phenylacetylene indicated decreased preference control, resulting in a 9.8:1 ratio (Fig. 1B). 4-Ethynylbenzonitrile reacted with organic azide **1a** at a comparable level to the thioalkyne **3a**, to form the corresponding triazoles in 34% yield with 1.6:1 ratio. Functional group-guided reactivity changes could likewise be observed in the competition assay between cyanoalkynes and thioalkynes, as illustrated in Fig. 1C. The participation of thioalkynes in the reaction increased in the order of decreasing electron density. 4-Cyano-triazole **5aa** was formed at an enhanced reactivity of 45.5:1, compared to 2.8:1 observed for thioalkynes **3f** and **3g**. Finally, we confirmed the reactivity preferences of cyanoalkynes, thioalkynes and terminal alkynes towards conjugation with benzyl azide under the NiAAC conditions (Fig. 1A–D). The direct comparison of relative reactivity of ynamides was difficult because two different ligands, Xantphos and dppbz, were used (see also Table 1, and the ESI†; Section IV, Scheme S1).

Table 2 NiAAC substrate scope[a]

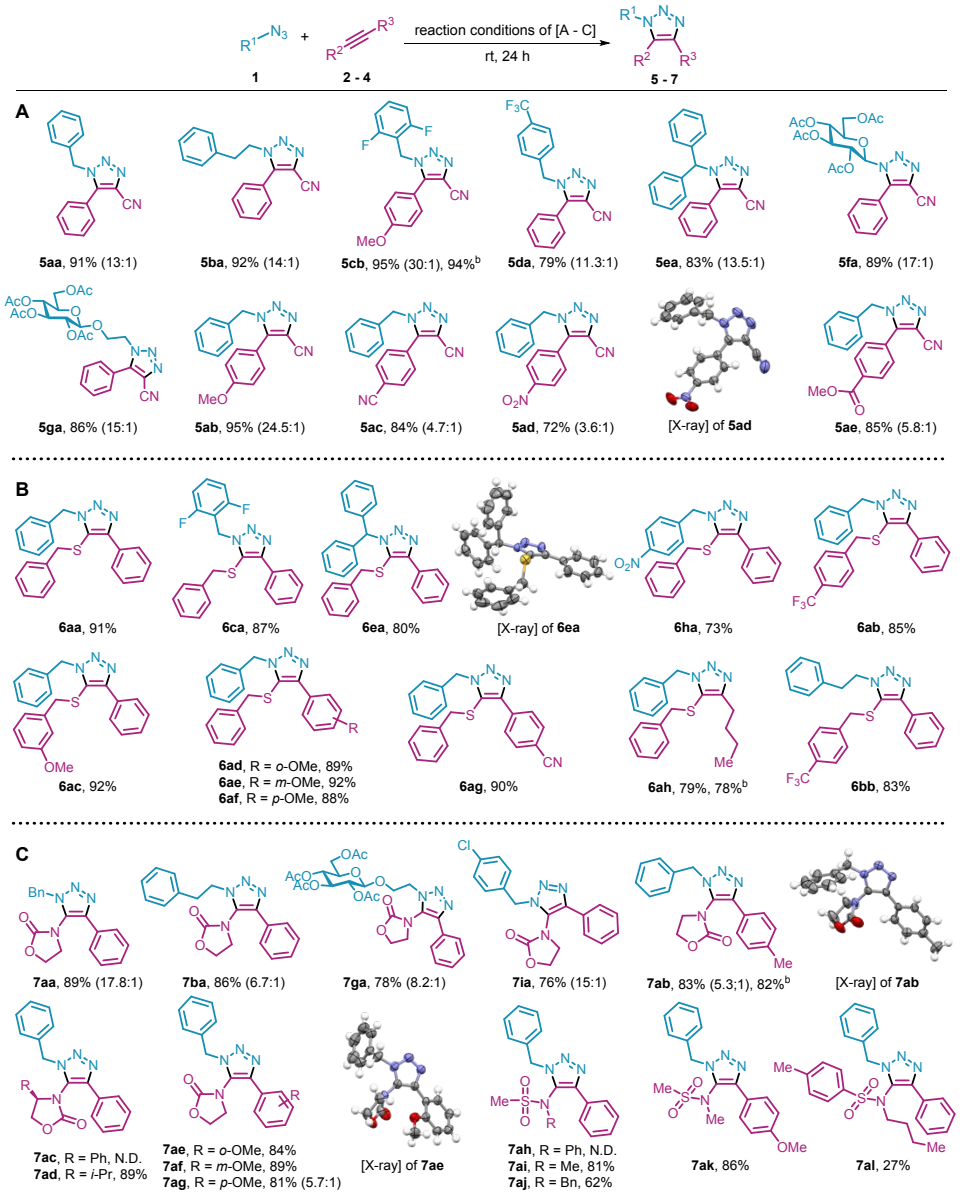

[a] Reaction conditions, (**A**) cyanoalkynes: **1** (0.38 mmol), **2** (0.46 mmol, 1.2 equiv), Cp_2Ni (10 mol %), Xantphos (10 mol %), Cs_2CO_3 (1.0 equiv) in DCM (2.0 mL) at rt under air for 24 h. (**B**) thioalkynes: **1** (0.38 mmol), **3** (0.46 mmol, 1.2 equiv), Cp_2Ni (20 mol %), Xantphos (20 mol %), Cs_2CO_3 (1.0 equiv) in DCM (2.0 mL). (**C**) ynamides: **1** (0.38 mmol), **4** (0.46 mmol, 1.2 equiv), Cp_2Ni (20 mol %), dppbz (20 mol %), Cs_2CO_3 (1.0 equiv) in toluene (2.0 mL). Isolated yields. The regioisomeric ratios are indicated in parentheses. [b] **1** (3 mmol) and **2–4** (3.6 mmol).

View Article Online
DOI: 10.1039/D0OB00579G

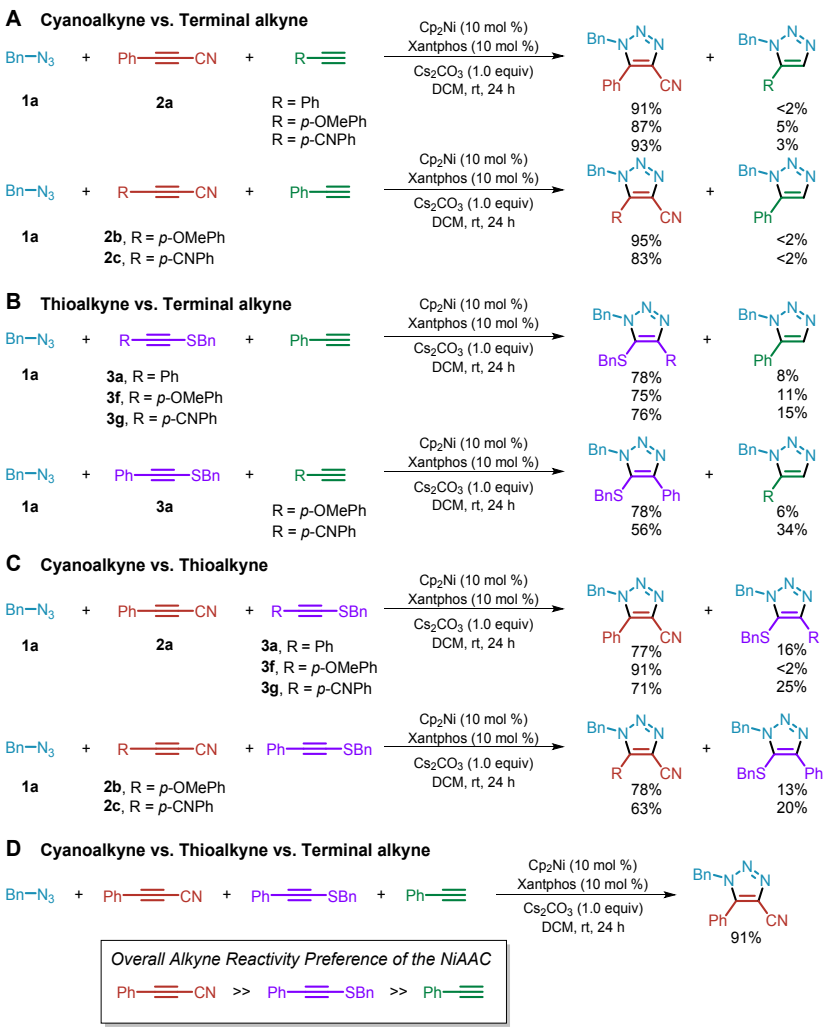

Fig. 1 Competition studies between unsymmetrical alkynes. (**A**) Cyanoalkyne vs. Terminal alkyne. (**B**) Thioalkyne vs. terminal alkyne. (**C**) Cyanoalkyne vs. thioalkyne. (**D**) Overall comparison. Reaction conditions: **1a** (0.38 mmol), competing alkynes (each 0.38 mmol, 1.0 equiv), Cp_2Ni (10 mol %), Xantphos (10 mol %), Cs_2CO_3 (1.0 equiv) in DCM (2.0 mL) at rt under air for 24 h. Isolated yields.

The distinct reactivity of the alkyne components allows for the development of a chemoselective click reaction strategy (Fig. 2). We conducted the NiAAC reactions by employing a solution of benzyl azide **1a**, cyanoalkyne **2a**, and phenylacetylene (Fig. 2A). Taking advantage of the reactivity preference for cyanoalkyne **2a**, the preferential formation of 4-cyano-1,2,3-triazole was observed, as also shown in Fig. 1A. Successive NiAAC reactions, as achieved by the addition of 1 equivalent of **1a**, furnished the corresponding 1,5-disubstituted 1,2,3-triazole from phenylacetylene in 82% isolated yield. This NiAAC chemoselective click strategy was also applicable to binary alkyne pairs (thioalkyne **3a** vs. phenylacetylene, as shown in Fig. 2B; cyanoalkyne **2a** vs. thioalkyne **3a** as shown in Fig. 2C). As the Xantphos ligand was partially oxidized during the first NiAAC (monitored by *in situ* NMR), the subsequent NiAAC proceeding with residual ligand gave a diminished yield of 48% of the 1,5-disubstituted 1,2,3-triazole from phenylacetylene, as shown in Fig. 2D.

With these results in hand, we constructed a mechanism that incorporates all experimental observations and conducted density functional theory (DFT)[38] calculations to quantitatively assess the energetic plausibility thereof. All calculations were performed at the M06[39]/6-31G**[40]/cc-pVTZ(-f)[41] level of theory implemented in Jaguar 9.1 suite of program[42] and details are given in the ESI† (Section VIII). Previously, we demonstrated experimentally that $Ni(Xantphos)_2$ can be formed *in situ* from a mixture of Xantphos and Cp_2Ni through EPR spectroscopic and HRMS studies.[26] Our calculations indicate that one Xantphos ligand can be readily dissociated to afford a linear 14-electron Ni(0)-d^{10} complex **A1**; its reaction with cyanoalkyne and benzyl azide substrates is outlined in Fig. 3A. The reaction energy profile is displayed in Fig. 3B. We considered that benzyl azide might bind to the nickel complex first, but found that process to have a barrier of 13.6 kcal/mol and unlikely to occur

View Article Online
DOI: 10.1039/D0OB00579G

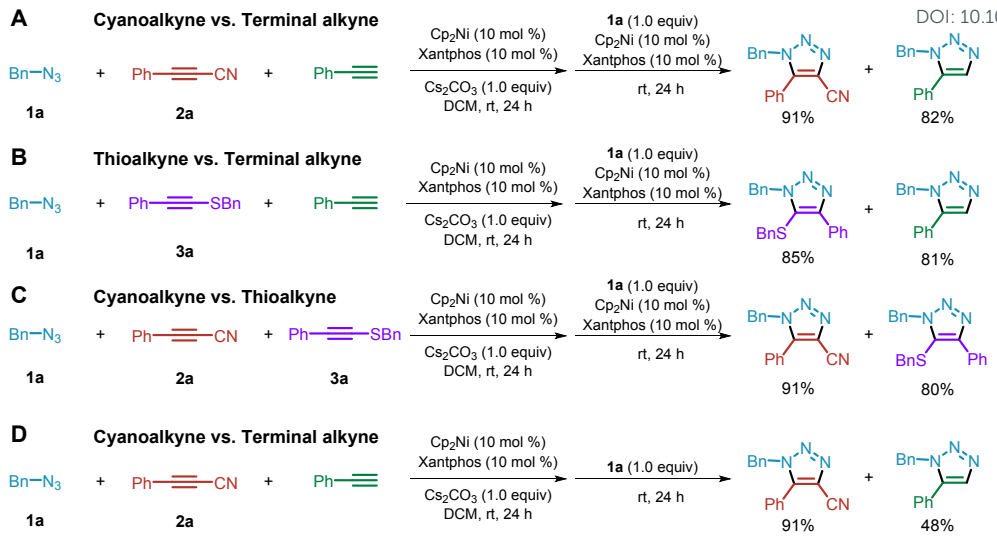

Fig. 2 Evaluation of the NiAAC as a chemoselective click strategy. (**A**) Cyanoalkyne vs. Terminal alkyne. (**B**) Thioalkyne vs. Terminal alkyne. (**C**) Cyanoalkyne vs. Thioalkyne. (**D**) Cyanoalkyne vs. Terminal alkyne. Reaction conditions: **1a** (0.38 mmol), two competing alkynes (each 0.38 mmol, 1.0 equiv), Cp_2Ni (10 mol %), Xantphos (10 mol %), Cs_2CO_3 (1.0 equiv) in DCM (2.0 mL) at rt under air for 24 h. Isolated yields. For the chemoselective click reactions, **1a** (1.0 equiv), Cp_2Ni (10 mol %), and Xantphos (10 mol %) were added to the reaction mixture, and stirring was continued for another 24 h.

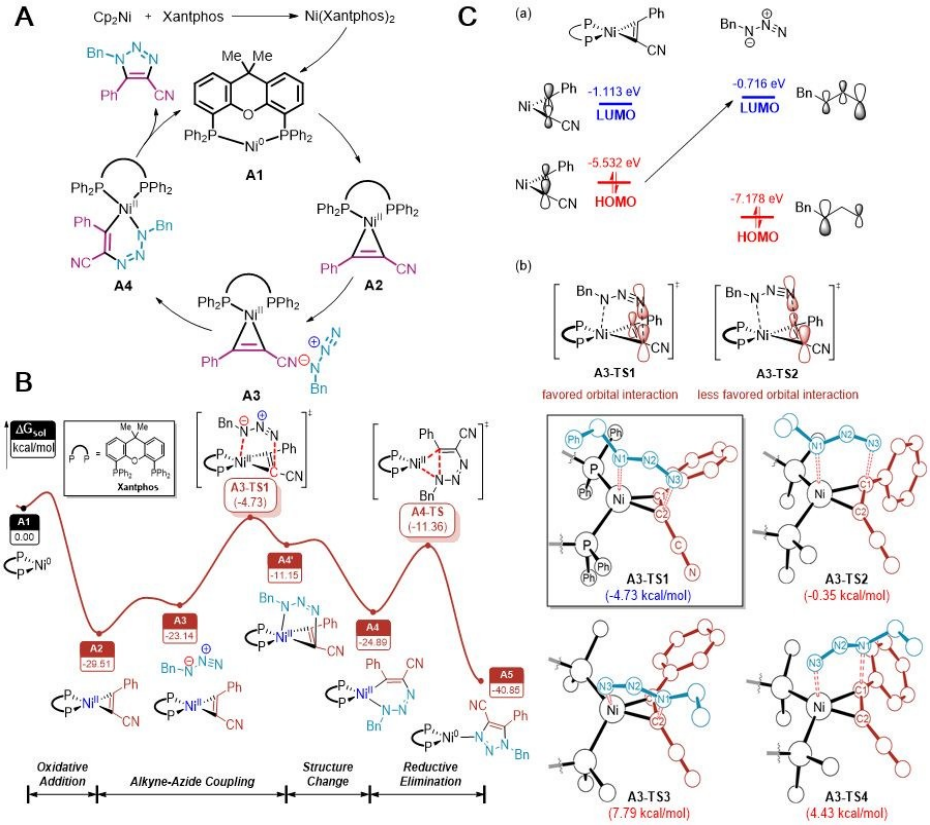

Fig. 3 Computational mechanistic studies in support of experimental results. (**A**) Proposed mechanism. (**B**) Free energy profile for the NiAAC reaction of the cyanoalkyne and benzyl azide substrates (Xantphos ligand is omitted for clarity). (**C**) Orbital Interactions. (a) Frontier molecular orbital diagram of the interaction between the nickellacycle **A2** and benzyl azide. (b) Orbital interactions in the C–N coupling transition states.

(see also the ESI†, Fig. S1). Instead, the productive reaction starts with a highly exergonic oxidative addition of the alkyne to give the Ni(II)-cyclopropene intermediate **A2** at –29.5 kcal/mol, which may be engaged by the azide substrate to furnish the adduct **A3** at –23.1 kcal/mol (Fig. 3B).

View Article Online
DOI: 10.1039/D0OB00579C

The subsequent cycloaddition that produces the nickellacycle **A4** is not only the most difficult step of the reaction with a barrier of at least 24.8 kcal/mol, but it also determines the regioselectivity. In principle, there are four possible transition states that will give two different triazole products, as shown in Fig. 3B. The frontier orbitals that govern the cyclization geometry are depicted in Fig. 3C(a). In the C–N coupling process, the nickellacycle **A2** acts as a nucleophile and its HOMO at –5.53 eV attacks the LUMO of benzyl azide at the N3 position where the coefficient of the LUMO is the largest. The other possible HOMO/LUMO interaction whereby the HOMO of benzyl azide at –7.18 eV attacks the LUMO of the **A2** at –1.11 eV has a larger energy gap and can therefore be ruled out. Consequently, the corresponding transition states **A3-TS3** and **A3-TS4** where the N1 of the benzyl azide nucleophilically attacks the **A2** were found to be 12.5 and 9.2 kcal/mol higher in energy, respectively, than **A3-TS1**. The transition state **A3-TS2** takes advantage of the same HOMO/LUMO interaction as **A3-TS1**, but the less nucleophilic phenyl-substituted C1 carbon is attacked. In the lowest energy transition state **A3-TS1**, the most nucleophilic cyano-substituted C2 carbon where the amplitude of the HOMO is greatest is matched with the most electrophilic terminal azide site, as illustrated in Fig. 3C(b). The predicted barrier of 24.8 kcal/mol is consistent with the mild conditions of the NiAAC.

The intermediate **A4'** resulting from the C–N coupling is severely distorted and undergoes ring-expansion readily to form the thermodynamically stable intermediate **A4** at –24.9 kcal/mol. This six-membered nickellacycle is poised to reductively eliminate the 1,4,5-trisubstituted 4-cyano-1,2,3-triazole product traversing the transition state **A4-TS** that is located at the 18.2 kcal/mol relative to the resting state **A2**. This reaction energy profile highlights the origin of regioselectivity in the generation of 1,4,5-trisubstituted 4-cyano-1,2,3-triazole products observed experimentally.

With the detailed mechanism of the NiAAC reaction in hand, we examined the chemoselectivity seen for the alkyne substrates. To study the chemoselectivity as a function of the electronic demand of the functional group, we augmented our calculations on the cyanoalkyne with a terminal alkyne and a thioalkyne, representing a non-functionalized and an electron-rich alkyne substrate, respectively. The NiAAC reactions of these substrates follow the same mechanism (see the ESI†; Figs. S2 and S3), and Fig. 4A(a) compares the cyclization step observed for the terminal alkyne with that of the cyanoalkyne. The terminal alkyne exhibits the same regioselectivity as cyanoalkyne for the cycloaddition, however the corresponding C–N coupling transition state **B3-TS1** is 7.7 kcal/mol higher in energy than **A3-TS1** and, similarly, the nickellacyclopropene intermediate **B2** located at –22.54 kcal/mol is 7 kcal/mol less stable than **A2**. These reaction profiles offer a simple explanation for the competition experiment summarized in Fig. 1A. Because the transition state **B3-TS1** is 2.9 kcal/mol higher than the reactant state, the cyclization competes with the reductive elimination from intermediate **B2** to re-generate the starting complex **A1**. The cyanoalkyne reactant does not suffer from this inefficiency and can hence outperform the terminal alkyne in a competition reaction. Frontier MO analysis visualizes the impact of the electron-withdrawing cyano functionality, as illustrated in Fig. 4A(b). The terminal alkyne-bound intermediate **B2** displays a smaller HOMO π orbital coefficient at the C2-position, with 55.6% composition at that site, whereas 60.4% is seen for the same site in **A2**. The electronic effect of cyano functionality directs the nucleophilic attack to the azide.

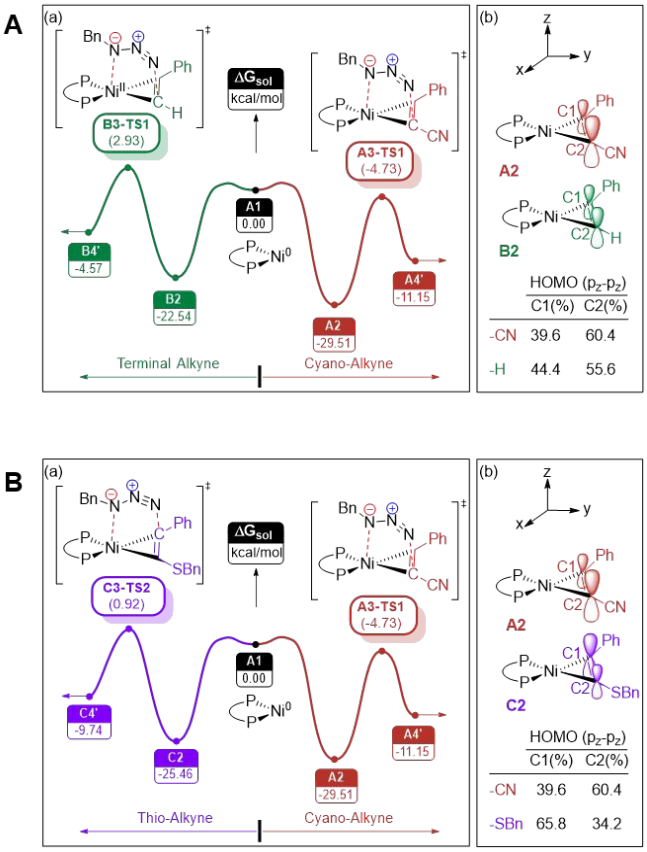

Fig. 4 Computational elucidation of chemo- and regioselectivity in the NiAAC. (**A**) Cyanoalkyne vs. terminal alkyne: (a) Free energy profile for the chemoselective step of the NiAAC reaction in the terminal alkyne and the cyanoalkyne, (b) The p_z-orbital coefficients of HOMO in the **A2** and **B2**. **(B)** Cyanoalkyne vs. thioalkyne: (a) Free energy profile for the chemoselective step of the NiAAC reaction in the thioalkyne and the cyanoalkyne. (b) The p_z-orbital coefficients of HOMO in the **A2** and **C2**.

Considering the frontier orbital concept discussed above, one can rationalize why the thioalkyne results in distinct regiochemistry and forms the 1,4,5-trisubstituted 5-thio-1,2,3-triazole product (Fig. 4B). Because the electron-donating ability of the thio-group renders the C1 carbon that carries the phenyl moiety the more nucleophilic site, we expect that the transition state **C3-TS2** in which the azide attacks the C1 carbon is lower in energy than **C3-TS1** (see also Fig. S3). Our calculations confirm this conceptual prediction precisely and we were able to locate **C3-TS2** at 0.9 kcal/mol, which is the lowest energy transition state with **C3-TS1** being at 5.6 kcal/mol. The frontier orbitals illustrate the inverted electronic structure in the p_z-orbital contributions to the HOMO of C1, summarized in Fig. 4B(b). The thio-substituent reduces the C2 p_z-orbital contribution to the HOMO notably to only 34.2% and increases

View Article Online
DOI: 10.1039/D0OB00579G

the C1 p_z-orbital contribution to 65.8%, which is a complete inversion of what was found in the cyanoalkyne substrate. Energetically, **C3-TS2** is 5.7 kcal/mol higher in energy than **A3-TS1**. Thus, the process leading to the preference for the cyanoalkyne reactant in the competition experiment discussed above is also applicable when thioalkyne and cyanoalkyne substrates compete. However, because the thioalkyne is more reactive, reflected in a barrier of cycloaddition that is ~2 kcal/mol lower than what was found for the terminal alkyne, thioalkyne cyclization is not entirely dominated by the cyanoalkyne reaction and minor amounts of thioalkyne cyclization products can be found in the competition reactions.

Conclusions

Nickel-catalyzed cycloaddition of organic azides and unsymmetrical alkynes was accomplished. The competing click chemistry was successfully established in a controlled and protection-group-free manner, featuring high levels of regio- and chemoselectivity, good functional group tolerance and mild reaction conditions. DFT calculations show that the cyclization step is the most demanding and rate-determining step. Ni-catalyst is capable of enhancing the electronic differences of the alkyne substrates by binding them via an oxidative addition process to the nickel center, leading to the reactivity- and selectivity preferences.

Conflicts of interest

There are no conflicts to declare.

Acknowledgements

This research was supported by the National Research Foundation of Korea (NRF) Grant (2018M1A2A2063341) funded by the Ministry of Science and ICT & Future Planning. M.-H.B. acknowledges support from Institute for Basic Science (IBS-R10-A1) in Korea.

Notes and references

1 *(a)* N. A. Afagh and A. K. Yudin, *Angew. Chem., Int. Ed.*, 2010, **49,** 262; *(b)* B. M. Trost, *Angew. Chem., Int. Ed.*, 1995, **34,** 259.
2 *(a)* N. De and E. J. Yoo, *ACS Catal.*, 2018, **8,** 48; *(b)* P. P. Painter, R. P. Pemberton, B. M. Wong, K. C. Ho and D. J. Tantillo, *J. Org. Chem.,* 2014, **79,** 432; *(c)* B. Engels and M. Christl, *Angew. Chem., Int. Ed.*, 2009, **48,** 7968; *(d)* K. N. Houk, J. Sims, C. R. Watts and L. J. Luskus, *J. Am. Chem. Soc.*, 1973, **95,** 7301.
3 *(a)* C. Wang, D. Ikhlef, S. Kahlal, J.-Y. Sailard and D. Astruc, *Coord. Chem. Rev.*, 2016, **316,** 1. *(b)* B. Heller and M. Hapke, *Chem. Soc. Rev.*, 2007, **36,** 1085*; (c)* Y. Ni and J. Montgomery, *J. Am. Chem. Soc.*, 2006, **128,** 2609; *(d)* P. A. Evans, J. E. Robinson, E. W. Baum and A. N. Fazal, *J. Am. Chem. Soc.*, 2002, **124,** 8782; *(e)* M. Lautens, W. Klute and W. Tam, *Chem. Rev.*, 1996, **96,** 49.
4 A. Marrocchi, A. Facchetti, D. Lanari, S. Santoro and L. Vaccaro, *Chem. Sci.*, 2016, **7,** 6298.
5 B. T. Worrell, J. A. Malik and V. V. Fokin, *Science*, 2013, **340,** 457.
6 J. E. Hein and V. V. Fokin, *Chem. Soc. Rev.*, 2010, **39,** 1302.
7 M. Meldal and C. W. Tornøe, *Chem. Rev.*, 2008, **108,** 2952.
8 C. W. Tornøe, C. Christensen and M. Meldal, *J. Org. Chem.*, 2002, **67,** 3057.
9 V. V. Rostovtsev, L. B. Green, V. V. Fokin and K. B. Sharpless, *Angew. Chem., Int. Ed.*, 2002, **41,** 2596.
10 P. Liu, R. J. Clark and L. Zhu, *J. Org. Chem.*, 2018, **83,** 5092.
11 P. Destito, J. R. Couceiro, H. Faustino, F. López and J. L. Mascareñas, *Angew. Chem., Int. Ed.*, 2017, **56,** 10766.
12 J. R. Johansson, T. Beke-Somfai, A. S. Stalsmeden and N. Kann, *Chem. Rev.*, 2016, **116,** 14726.
13 S. Ferrini, J. Z. Chandanshive, S. Lena, M. Comes Franchini, G. Guanyin, A. Tafi and M. Taddei, *J. Org. Chem.*, 2015, **80,** 2562.
14 J. R. Johansson, P. Lincoln, B. Norden and N. Kann, *J. Org. Chem.*, 2011, **76,** 2355.
15 B. C. Boren, S. Narayan, L. K. Rasmussen, L. Zhang, H. Zhao, Z. Lin, G. Jia and V. V. Fokin, *J. Am. Chem. Soc.*, 2008, **130,** 8923.
16 L. Zhang, X. Chen, P. Xue, H. H. Y. Sun, I. D. Williams, K. B. Sharpless, V. V. Fokin and G. Jia, *J. Am. Chem. Soc.*, 2005, **127,** 15998.
17 W. Song, N. Zheng, M. Li, J. He, J. Li, K. Dong, K. Ullah and Y. Zheng, *Adv. Synth. Catal.*, 2019, **361,** 469.
18 W. Song, N. Zheng, M. Li, K. Ullah and Y. Zheng, *Adv. Synth. Catal.*, 2018, **360,** 2429.
19 W. Song, N. Zheng, M. Li, K. Dong, J. Li, K. Ullah and Y. Zheng, *Org. Lett.*, 2018, **20,** 6705.
20 Y. Liao, Q. Lu, G. Chen, Y. Yu, C. Li and X. Huang, *ACS Catal.*, 2017, **7,** 7529.
21 R. Chen, L. Zeng, Z. Lai and S. Cui, *Adv. Synth. Catal.*, 2019, **361,** 989.
22 W. Song and N. Zheng, *Org. Lett.*, 2017, **19,** 6200.
23 S. Ding, G. Jia and J. Sun, *Angew. Chem., Int. Ed.*, 2014, **53,** 1877.
24 Q. Luo, G. Jia, J. Sun and Z. Lin, *J. Org. Chem.*, 2014, **79,** 11970.
25 E. Rasolofonjatovo, S. Theeramunkong, A. Bouriaud, S. Kolodych, M. Chaumontet and F. Taran, *Org. Lett.*, 2013, **15,** 4698.
26 W. G. Kim, M. E. Kang, J. B. Lee, M. H. Jeon, S. Lee, J. Lee, B. Choi, P. M. S. D. Cal, S. Kang, J.-M. Kee, G. J. L. Bernades, J.-U. Rohde, W. Choe and S. Y. Hong, *J. Am. Chem. Soc.*, 2017, **139,** 12121.
27 N. Münster, P. Nikodemiak and U. Koert, *Org. Lett.*, 2016, **18,** 4296.
28 R. R. Ramsubhag and G. B. Dudley, *Org. Biomol. Chem.*, 2016, **14,** 5028.
29 M. Z. C. Hatit, C. P. Seath, A. J. B. Watson and G. A. Burley, *J. Org. Chem.*, 2017, **82,** 5461.
30 I. E. Valverde, F. Lecaille, G. Lalmanach, V. Aucagne and A. F. Delmas, *Angew. Chem., Int. Ed.*, 2012, **51,** 718.
31 V. Aucagne and D. A. Leigh, *Org. Lett.*, 2006, **8,** 4505.
32 C. P. Seath, G. A. Burley and A. J. B. Watson, *Angew. Chem., Int. Ed.*, 2017, **56,** 3314.
33 M. Z. C. Hatit, J. C. Sadler, L. A. McLean, B. C. Whitehurst, C. P. Seath, L. D. Humphreys, R. J. Young, A. J. B. Watson and G. A. Burley, *Org. Lett.*, 2016, **18,** 1694.
34 A. A. Kislukhin, V. P. Hong, K. E. Breitenkamp and M. G. Finn, *Bioconjugate Chem.*, 2013, **24,** 684.
35 Z. Yuan, G.-C. Kuang, R. J. Clark and L. Zhu, *Org. Lett.*, 2012, **14,** 2590.
36 R. Chung, A. Vo, V. V. Fokin and J. E. Hein, *ACS Catal.*, 2018, **8,** 7889.
37 P. W. N. M. van Leeuwen, P. C. J. Kamer, J. N. H. Reek and P. Dierkes, *Chem. Rev.*, 2000, **100,** 2741.
38 R. G. Parr and Y. Weitao, *Density-Functional Theory of Atoms and Molecules*, Oxford University Press, New York, 1994.
39 Y. Zhao and D. G. Truhlar, *Theor. Chem. Acc.*, 2008, **120,** 215.

View Article Online
DOI: 10.1039/D0OB00579G

40 R. Ditchfield, W. J. Hehre and J. A. Pople, *J. Chem. Phys.*, 1971, **54,** 724.
41 T. H. Dunning, *J. Chem. Phys.*, 1989, **90,** 1007.
42 A. D. Bochevarov, E. Harder, T. F. Hughes, J. R. Greenwood, D. A. Braden, D. M. Philipp, D. Rinaldo, M. D. Halls, J. Zhang and R. A. Friesner, *Int. J. Quantum Chem.*, 2013, **113,** 2110.